

Tidal Variability in the Water Quality of an Urbanized Estuary

J. L. DiLORENZO^{1,*}, R. J. FILADELFO², C. R. SURAK¹, H. S. LITWACK¹, V. K. GUNAWARDANA¹,
and T. O. NAJARIAN¹

¹ *Najarian Associates, One Industrial Way West, Eatontown, New Jersey 07724*

² *Center for Naval Analyses, 4825 Mark Center Drive, Alexandria, Virginia 22311*

ABSTRACT: Tide and water quality data were collected concurrently in the Hackensack River estuary (HRE), a tidal tributary of the New York-New Jersey Harbor estuary. Harmonic analyses of tidal elevation data indicate that HRE tides are predominantly semidiurnal, though modulated by diurnal and fortnightly components. Nearly uniform tidal ranges (averaging approximately 1.6 m) were observed at three stations within the HRE. Periodogram estimates reveal significant tidal variability for the water quality parameter $\text{NH}_4\text{-N}$ under dry-weather conditions. Lag correlation analyses associate $\text{NH}_4\text{-N}$ concentration variations with water level fluctuations. Longitudinal profile plots for $\text{NH}_4\text{-N}$ reveal a consistent pattern of tidal translations, with peak concentrations oscillating about a major wastewater discharger. These analyses suggest that the distribution of $\text{NH}_4\text{-N}$ concentration in the HRE is controlled primarily by major point source loadings and horizontal advection. A simplified, one-dimensional model is used to describe this distribution. Effects of tidal variability in masking water quality status and weak trends are also analyzed. These analyses highlight the potential importance of short-term water quality variability in tidal estuaries where concentration gradients are large.

Introduction

Estuarine water quality varies in response to physical transport processes. Tidal advection periodically displaces dissolved and suspended matter in estuaries, altering constituent concentrations over dominant tidal periods. Tidal shears disperse pollutants and reduce peak concentrations near pollutant sources (Geyer and Signell 1992). Mean currents induced by freshwater discharges sweep water quality constituents seaward and sharpen frontal gradients. In some stratified estuaries, tidal stirring induces complete vertical mixing of water quality constituents around high water, except during neap tides (Simpson et al. 1990; Uncles 2002). Fortnightly tidal fluctuations may modulate the vertical density structure and associated gravitational circulation patterns that transport buoyant substances offshore and deeper dissolved substances inshore (Sharples and Simpson 1993; Uncles 2002). Meteorological forcings induce variability at subtidal time scales and can act as effective flushing agents in estuaries (Goodrich 1988).

Besides physical transport processes, pollutant sources such as urban runoff, municipal dischargers, industrial dischargers, combined sewer overflows, landfills, and atmospheric deposition induce complex patterns of water quality variability in urbanized estuaries. Many conventional water quality constituents are transformed in estuaries, via internal biogeochemical processes, from one storage form to another depending upon availability of nu-

trients, heat, and light. Emphasis has been placed historically on water quality variability at subtidal time scales (weekly, seasonal, annual) in recognition of such complex interactions and their associated time scales. Short-term (hourly) water quality variability can be substantial and, in some cases, comparable to variability at longer time scales (Cloern et al. 1989; Hubertz and Cahoon 1999; Sanderson and Taylor 2003). This is particularly the case in estuaries having both large horizontal concentration gradients (near major point sources) and moderate or large tidal excursions.

Present knowledge does not allow us to determine, a priori, whether tides are dominant controls on the water quality of a particular estuary. This lack of knowledge may hamper the efficient design of water quality monitoring programs and the detection of weak water quality trends. The goals of this study are to assess both tides and tidal variability in the water quality of an urbanized estuary and to assess the influence of this tidal variability on the detection of water quality trends. A set of concurrent tidal elevation, current, and water quality measurements collected several years ago in the Hackensack River estuary (HRE) provides an excellent, readily available data set for these purposes.

The HRE is a narrow inland extension of the New York Harbor complex. From its head of tide at the Oradell Dam, the HRE extends about 35 km southward to its confluence with the Upper Newark Bay and the Passaic River (Fig. 1). The HRE has average centerline depths of 7.6 m and a maximum width of 600 m.

* Corresponding author: tele: 732/389-0220; fax: 732/389-8546; e-mail: dilorenzo@najarian.com

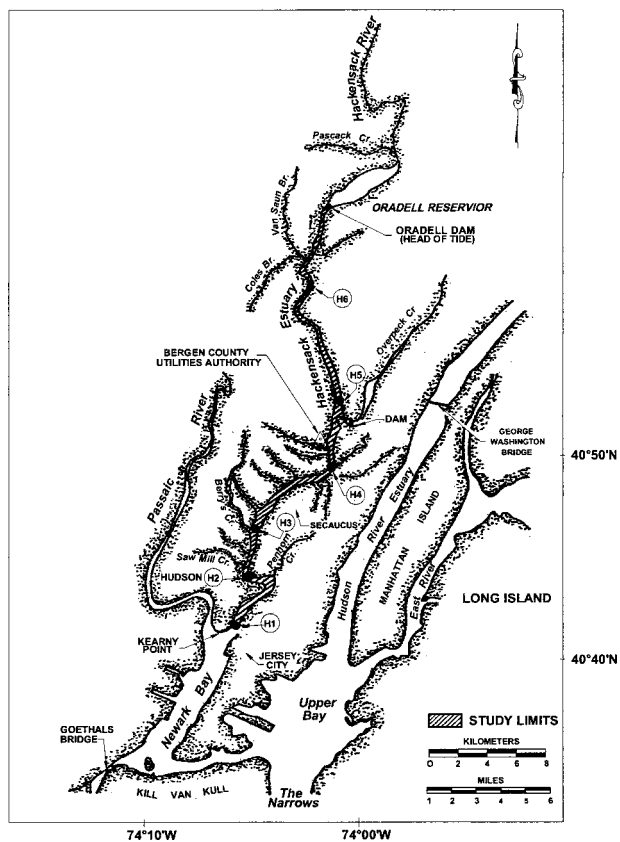


Fig. 1. Location of Hackensack River Estuary, adjacent waterways and data collection locations.

The HRE drains an urbanized, 217.6-km² watershed dominated by the Hackensack Meadowlands, an 80.9-km² area of tidal wetlands located in the lower HRE. The upper, nontidal Hackensack River drains a comparable (292.7 km²) watershed area and terminates at a large impoundment, the Oradell Reservoir. Due to large reservoir withdrawals, the long-term average freshwater inflow to the HRE (10.9 m³ s⁻¹) is small relative to the mean tidal discharge at the mouth (approximately 1,200 m³ s⁻¹; Najarian Associates 1990). Freshwater inflows are contributed largely (33% on average) by a single municipal discharger, the Bergen County Utility Authority's (BCUA) wastewater treatment plant (at km 20). The average ratio of tidal to freshwater flows (approximately 110) is reflected in the low vertical salinity stratification (typically < 1 psu) reported for this system (Najarian Associates 1990).

Over the years, HRE water quality has been influenced by urbanization and industrialization within its watershed, reservoir withdrawals, and tidal exchange with adjacent, coastal waterways. This includes the adjacent Passaic River Estuary, whose watershed is approximately 11 times larger than

HRE. Due to its limited freshwater inflow and indirect communication with the open sea, the HRE is inherently susceptible to local pollution sources, including wastewater dischargers, storm sewers, local landfills, contaminated sediment deposits, upstream drawdowns, atmospheric depositions, and tidal exchange with Newark Bay. The collective inputs from all of these sources have degraded HRE water quality and sediment quality (Squibb et al. 1991). Though some water quality improvements were reported in the early 1970s, no significant overall trends in HRE water quality were reported for the period 1971–1988 (Keller et al. 1990). This overall pattern contrasts water quality improvements observed in the adjacent Hudson River estuary (Brosnan and O'Shea 1996).

Sampling Methods

Tidal and water quality data were collected concurrently in the HRE during the spring and summer of 1988. From April 1 through September 30, 1988, continuous tidal elevations were measured with TDR-3A tide recorders at stations H1, H3, and H5 (Fig. 1). These subsurface, pressure-sensing units were installed on rigid mounting frames attached to local bulkhead structures. The measured tidal elevations were referenced to a common vertical datum (NGVD-1929). Mid depth current velocities were measured at location H1 using an Endeco type-105 in situ recording current meter. The sampling interval for sea level and current was 0.25 h.

Discrete water quality samples were also collected manually at stations H1 (km 2.1), H2 (km 8.2), H3 (km 11.4), H4 (km 17.3), H5 (km 21.9), and H6 (km 28.8; automatic water quality sampling equipment was deemed impractical for this urbanized site). To isolate tidal variability, we analyzed water samples collected during a dry-weather period July 11–18, 1988. Rainfall totals (measured at Newark International Airport) were below 0.63 cm (0.25 in) during July 1–16, followed by a single rainfall event of nearly 2.5 cm on July 17. For this period, the U.S. Geological Survey reported typical daily Hackensack River discharges of 0.03 m³ s⁻¹ near the head of tide at New Milford (drainage area of 303 km²).

The discrete water quality samples were analyzed in the laboratory according to standard U.S. Environmental Protection Agency methods for chemical analysis (U.S. EPA 1983). While these samples were analyzed for several conventional water quality parameters, we focus our analyses on the parameter NH₄-N due to the presence of a large domestic discharger (BCUA). The sampling interval for NH₄-N concentration was 2 h at station H1 and 3 h at all other stations. On some intermittent oc-

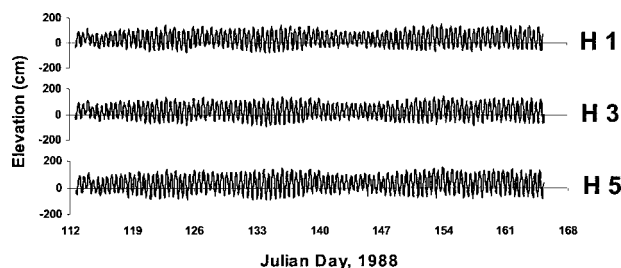


Fig. 2. Tidal elevations at station H1 (km 2.1), H3 (km 11.4), H5 (km 22.0).

cations, samples were not collected at the specified times.

Results

TIDAL FLUCTUATIONS

The observed tidal ranges at stations H1, H3, and H5 are nearly uniform, averaging about 160 cm throughout the sampled portion of the HRE (Fig. 2). Tidal fluctuations at station H5 (km 22.0) lag those at station H1 (km 2.1) by approximately 0.7 h (Fig. 3). Observed currents near the mouth (km 2.1) indicate nearly symmetrical flooding and ebbing tides, with typical amplitudes of about 60 cm s^{-1} . These current fluctuations lead observed tidal elevation variations by approximately one quarter of a tidal cycle, with both high water and low water occurring throughout the sampled portion of the estuary near the recorded slack-water intervals (characteristic of near standing wave tides).

Harmonic analyses of the observed water levels (Table 1) reveal predominantly semidiurnal tides. The principal lunar semidiurnal tidal constituent (M_2 tide) has the largest tidal amplitude at all stations. Diurnal components also contribute to HRE tidal variability, as indicated by an F ratio of 0.19. The tidal records indicate significant spring-neap

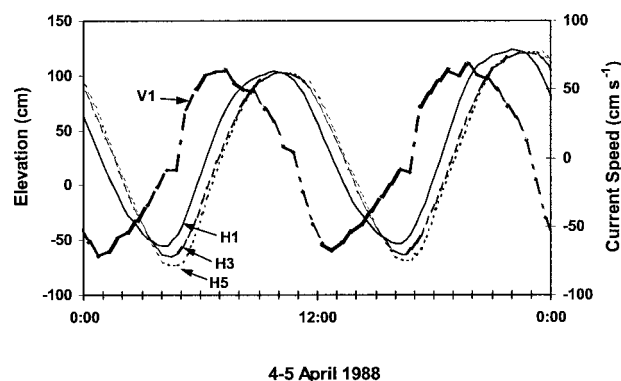


Fig. 3. Observed tidal elevations at stations H1 (km 2.1), H3 (km 11.4) and H5 (km 22.0), and tidal currents at station H1 on April 4, 1988.

modulations. Some overtide generation is apparent, as the computed $M_4:M_2$ ratio ranges from about 6% to 7%.

TIDAL INFLUENCES ON WATER QUALITY

To characterize tidal variability in HRE water quality, we plotted concurrent time series of tidal elevation and $\text{NH}_4\text{-N}$ concentration at stations where both variables were sampled: H1, H3, and H5 (Fig. 4). Observed $\text{NH}_4\text{-N}$ concentrations fluctuated, over semidiurnal periods, at each station during the selected dry-weather period. At the site located 2 km up-estuary from BCUA (H5), $\text{NH}_4\text{-N}$ levels varied between 3–7 mg l^{-1} , with peak concentrations occurring around high water. Somewhat lower peak $\text{NH}_4\text{-N}$ concentrations (approximately 5 mg l^{-1} or less) occurred around low water at station H3 located approximately 8 km down-estuary from BCUA. At the station located closest to the mouth (i.e., H1 at km 2.1), $\text{NH}_4\text{-N}$ concentrations were comparatively stable, varying from 1 to 2 mg l^{-1} , with peak concentrations also around low water.

TABLE 1. Harmonic analysis results at each tide gauge station for the period of April 23–May 21, 1988.

| Constituent | Period (h) | Station H1 (km 2.3) | | Station H3 (km 11.4) | | Station H5 (km 22.0) | |
|-------------|------------|---------------------|-------------|----------------------|-------------|----------------------|-------------|
| | | Ampl. (cm) | Phase (GMT) | Ampl. (cm) | Phase (GMT) | Ampl. (cm) | Phase (GMT) |
| M_2 | 12.42 | 73.9 | 19.0 | 76.0 | 35.8 | 80.4 | 39.4 |
| S_2 | 12.00 | 14.0 | 33.2 | 13.5 | 56.5 | 14.2 | 61.3 |
| N_2 | 12.66 | 12.3 | 176.2 | 13.0 | 199.0 | 13.8 | 203.5 |
| K_1 | 23.93 | 12.6 | 166.7 | 12.9 | 179.1 | 13.4 | 179.2 |
| O_1 | 25.82 | 6.8 | 181.1 | 6.5 | 197.0 | 6.9 | 200.5 |
| MSF | 354.37 | 4.4 | 132.5 | 4.5 | 129.3 | 3.4 | 131.0 |
| M_4 | 6.21 | 4.4 | 283.3 | 4.3 | 285.2 | 5.5 | 290.1 |
| P_1 | 24.07 | 4.2 | 167.8 | 4.3 | 180.5 | 4.4 | 180.8 |
| K_2 | 11.97 | 3.8 | 34.4 | 3.7 | 29.0 | 3.9 | 33.9 |
| NU_2 | 12.63 | 2.8 | 12.4 | 2.9 | 193.2 | 3.1 | 196.3 |
| MS_4 | 6.10 | 2.5 | 250.8 | 3.3 | 274.7 | 4.0 | 283.2 |
| M_6 | 4.14 | 2.7 | 174.7 | 1.7 | 182.4 | 2.6 | 196.8 |
| F ratio* | | 0.19 | | 0.19 | | 0.19 | |

* F ratio = $(K_1 + O_1)/(M_2 + S_2 + N_2)$.

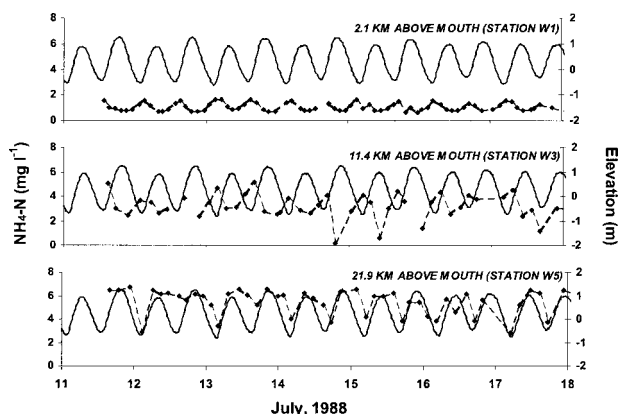


Fig. 4. Surface $\text{NH}_4\text{-N}$ time series at stations H1 (upper panel), H3 (middle panel) and H5 (lower panel) over the selected dry-weather period (July 11–18, 1988). Superimposed on each plot are corresponding tidal elevations (solid curves).

We plotted mean longitudinal profiles of $\text{NH}_4\text{-N}$ (Fig. 5) from data collected at all of the stations (H1–H6) around slack tide. This revealed a consistent pattern of tidal translations over this period, with the mean low-slack profile displaced down-estuary relative to the corresponding high-slack profile. This pattern likely results from several factors: BCUA is the major $\text{NH}_4\text{-N}$ source during dry-weather periods, typical effluent $\text{NH}_4\text{-N}$ concentrations of 17 mg l^{-1} exceed typical background concentrations of approximately 1 mg l^{-1} at the mouth, limited freshwater inflows to the estuary are contributed largely by BCUA during dry-weather periods, and tidal excursions are moderate in the HRE.

To quantify tidal forcing on $\text{NH}_4\text{-N}$ concentration, we applied lagged correlation analysis techniques to the observed data. We correlated sea level with $\text{NH}_4\text{-N}$ concentration at stations H1, H3,

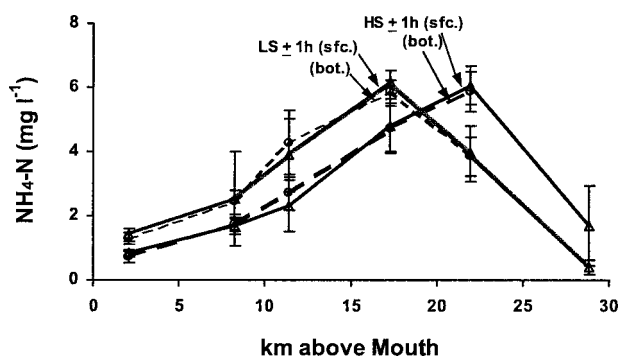


Fig. 5. Average longitudinal profiles of $\text{NH}_4\text{-N}$ concentration during the selected dry-weather period (July 11–18, 1988). Solid curves represent time-averages of surface samples collected around low-slack (LS) and high-slack (HS) tide; adjacent dashed curves represent corresponding profiles for bottom samples. Error bars indicate one sample standard deviation.

TABLE 2. Lag correlations between $\text{NH}_4\text{-N}$ concentrations and tidal elevations (bold type where significant at 95% level).

| Lag (h) | H1 | H3 | H5 |
|---------|---------------|---------------|--------------|
| 0 | -0.646 | -0.654 | 0.66 |
| 1 | -0.816 | -0.735 | 0.693 |
| 2 | -0.797 | -0.584 | 0.514 |
| 3 | -0.579 | -0.298 | 0.224 |

and H5. Note that the water level and water quality observations were not exactly concurrent. Since water levels were measured every 15 min, while $\text{NH}_4\text{-N}$ concentrations were recorded at time intervals of 2–3 h, we decimated the sea level data to correspond with the times of water quality measurements. Because sea levels were recorded every 15 min, this decimation yielded sea level observations within 8 min (or less) of the corresponding water quality measurement (or within 8 min of the appropriate lag). Table 2 shows the resulting lag correlations. Note that a 1-h lag implies that the constituent concentrations lag water levels by 1 h.

At station H5 (km 22.0), located about 2 km above BCUA, there is significant positive correlation at a lag of 1 h. $\text{NH}_4\text{-N}$ increases as the water surface rises (i.e., during flooding tides), suggesting an influence of treatment plant discharges. Results at stations H3 and H1 (located 8 and 18 km, respectively, below BCUA) indicate significant negative correlations at a lag of about 1 h. $\text{NH}_4\text{-N}$ concentration increases as the water surface falls (during ebbing tides), again suggesting an influence of discharges from BCUA.

Using standard spectral techniques, we computed periodogram estimates for $\text{NH}_4\text{-N}$ concentration at stations H3 and H5 (Fig. 6). These periodograms compare the relative proportion of the sample variance associated with both nontidal and tidal frequencies over a resolution bandwidth of 0.125 to 4 cycle d^{-1} (periods 6 h to 8 d). Some

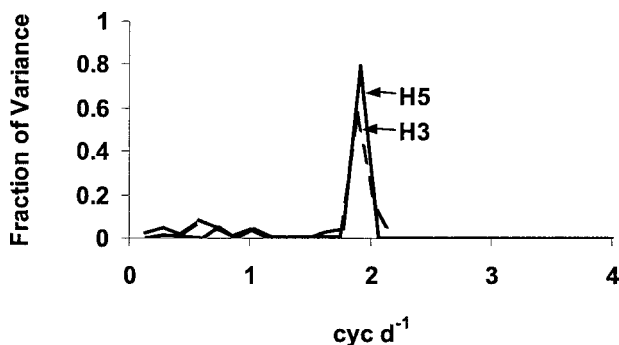


Fig. 6. Periodograms for $\text{NH}_4\text{-N}$ concentration at stations H3 and H5. Peaks at 2 cyc d^{-1} correspond to semi-diurnal variability; peaks at 1 cyc d^{-1} correspond to diurnal variability.

interpolation was necessary to compute these estimates.

At station H5, the fraction of variance in $\text{NH}_4\text{-N}$ concentration associated with the semidiurnal tidal period is 79.9%. At station H3, 57.9% of the variance in $\text{NH}_4\text{-N}$ is associated with the semidiurnal tidal period. These results indicate that tides are significant controls on observed $\text{NH}_4\text{-N}$ concentration in the HRE.

Discussion

CONCEPTUAL MODEL

The graphical, statistical, and spectral analyses described above suggest that longitudinal tidal advection is an important process controlling the $\text{NH}_4\text{-N}$ distribution in the HRE. Additional transport processes that influence the $\text{NH}_4\text{-N}$ distribution are longitudinal dispersion and longitudinal advection by the mean (freshwater discharge) flow. Important biochemical processes likely include nitrification, a transformation of $\text{NH}_4\text{-N}$ to $\text{NO}_2\text{-N}$ and $\text{NO}_3\text{-N}$. A very simple one-dimensional model for $\text{NH}_4\text{-N}$ variability (after Harleman 1971) is applied:

$$\frac{\partial C}{\partial t} + U \frac{\partial C}{\partial x} = E_L \frac{\partial^2 C}{\partial x^2} - kC \quad (1)$$

where C is the $\text{NH}_4\text{-N}$ concentration, t represents time, x is the longitudinal distance from the discharge, E_L is the longitudinal dispersion coefficient, k is the nitrification rate, and U is the longitudinal velocity component. The latter is assumed to consist of a steady freshwater flow (U_f) and a tidally varying component:

$$U(t) = U_f + U_T \sin \frac{2\pi t}{T} \quad (2)$$

where U_T is the tidal velocity amplitude and T is the tidal period. This simple model assumes a point source discharge into an infinite and uniform estuarine channel, and a continuous mass loading starting at time $t = \tau$. The integral solution to these equations is:

$$\frac{C}{C_o} = \int_0^t \frac{U_f}{\sqrt{4\pi E_L(t-\tau)}} \times \exp \left\{ \left[- \left[x - U_f(t-\tau) + \frac{U_T}{\omega} (\cos \omega t - \cos \omega \tau) \right]^2 \right] \div [4E_L(t-\tau)] - k(t-\tau) \right\} d\tau \quad (3)$$

where the peak reference concentration, C_o , is defined as the average effluent concentration (C_e) multiplied by the ratio of the effluent flow (Q_e) to the net freshwater discharge (Q_f):

$$C_o = \frac{Q_e C_e}{Q_f} \quad (4)$$

The conceptual model is applied with the following representative input values: a tidal period of 12.42 h, an assumed nitrification rate of 0.1 d^{-1} , an average effluent $\text{NH}_4\text{-N}$ concentration of 17 mg l^{-1} (based on an average of limited discharge monitoring data available for the selected period); an average effluent flow of $2.8 \text{ m}^3 \text{ s}^{-1}$; an average (dry-weather) freshwater flow of $3.3 \text{ m}^3 \text{ s}^{-1}$; a computed peak reference concentration of 14.5 mg l^{-1} (Eq. 4), an average discharge velocity (U_f) of 0.006 m s^{-1} , and an estimated tidal current speed of 0.32 m s^{-1} . The latter is estimated based on the $\text{NH}_4\text{-N}$ profile displacement of about 4.6 km and the tidal excursion (TE) relation:

$$\begin{aligned} \text{TE} &= \frac{U_T T}{\pi} = \frac{(0.32 \text{ m s}^{-1})(44,712 \text{ s})}{3.14159} \\ &= 4600 \text{ m} \end{aligned} \quad (5)$$

The longitudinal dispersion coefficient (assumed constant) is estimated (Harleman 1971) based on the Mannings n value, the current speed, and the hydraulic radius, R_h :

$$\begin{aligned} E_L &= 77nUR_h^{5/6} \\ &= 77(0.028)(0.32 \text{ m s}^{-1})(7 \text{ m}) \\ &= 4.8 \text{ m}^2 \text{ s}^{-1} \end{aligned} \quad (6)$$

Harleman (1971) suggests increasing this coefficient to approximately twice this value for an estuary that has channel bends and irregularities; a value of $10 \text{ m}^2 \text{ s}^{-1}$ was selected for the HRE.

With these representative inputs, the model solution was integrated numerically to reach a steady state (at $t = 150$ tidal cycles). Simulated longitudinal profiles for both high-slack and low-slack tide are displayed in Fig. 7 (upper left panel). Note that the abscissa in this plot is the distance from the discharge expressed in tidal excursions units (where $1 \text{ TE} = 4.6 \text{ km}$).

The overall shape of the simulated profiles for this case (Fig. 7, upper left panel) is explained as follows. Due to the continuous discharge over many tidal cycles, a buildup of relatively high concentrations occurs in the vicinity of the discharge (BCUA). These elevated levels are: translated up-estuary or down-estuary by the semidiurnal tide, spread longitudinally by dispersive processes, steadily advected down-estuary by the mean flow, and diminished (over time and during down-estu-

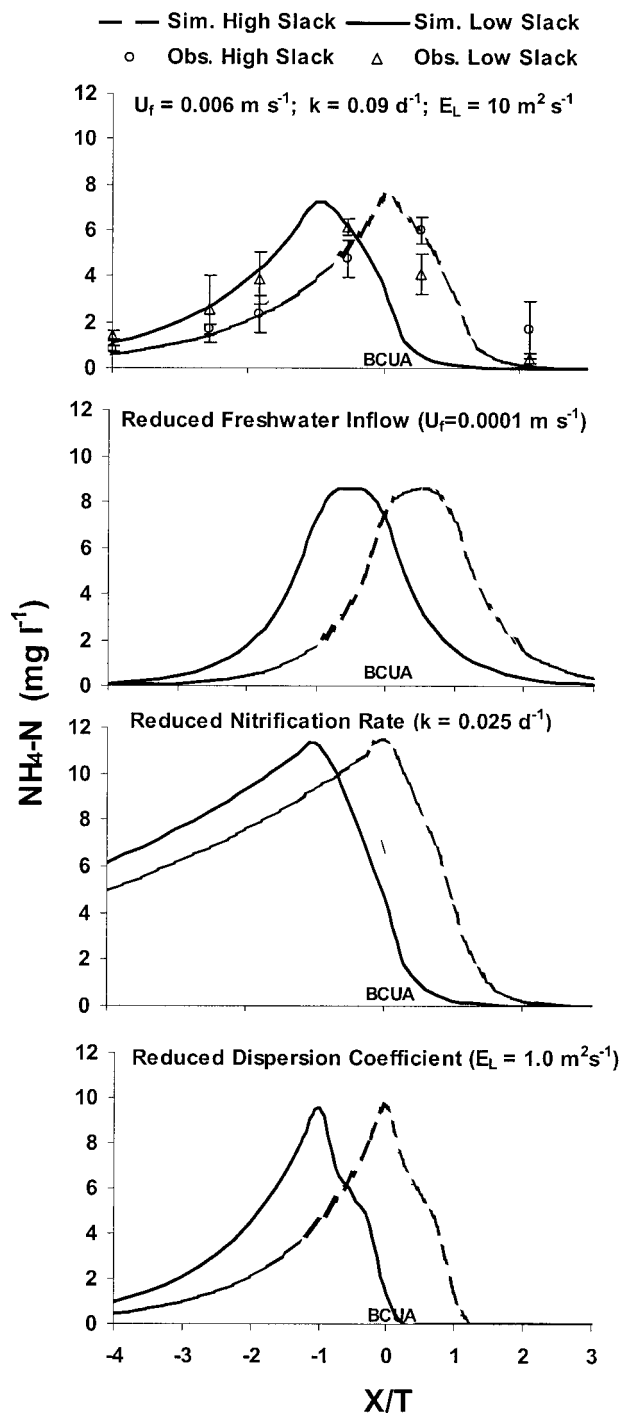


Fig. 7. Simulated longitudinal $\text{NH}_4\text{-N}$ profile plots for the selected dry-weather period (July 11–18, 1988). Horizontal distance from BCUA discharge plotted in units of 1 tidal excursion (TE) where 1 TE = 4.6 km. Panel (a): comparison of observed and simulated $\text{NH}_4\text{-N}$ profiles for $U_f = 0.006 \text{ m s}^{-1}$; $k = 0.09 \text{ d}^{-1}$; and $E_L = 10 \text{ m}^2 \text{ s}^{-1}$. Error bars indicate 1 sample standard deviation. Panel (b): effect of reduced freshwater inflow (i.e., $U_f = 0.0001 \text{ m s}^{-1}$). Panel (c): effect of reduced nitrification rate (i.e., $k_d = 0.025 \text{ d}^{-1}$). Panel (d): effect of reduced dispersion coefficient (i.e., $E_L = 1.0 \text{ m}^2 \text{ s}^{-1}$).

ary travel) by nitrification. The simulated profiles are asymmetrical about the origin (BCUA) since advection by the mean (freshwater) flow is always directed down-estuary. Without a significant freshwater inflow, the simulated profiles would be symmetrical about BCUA (e.g., Fig. 7, upper right panel).

The prescribed nitrification rate is a sensitive model parameter. An approximate 4-fold reduction in the selected rate would significantly elevate simulated concentrations that extend down-estuary from BCUA (Fig. 7, lower left panel). This suggests that nitrification is an important control, and that uncertainty in this parameter may significantly reduce model accuracy. Less sensitive, but important, is the prescribed longitudinal dispersion coefficient. A 10-fold decrease in the selected coefficient value results in locally narrowed and elevated peaks (Fig. 7, lower right panel).

As illustrated (Fig. 7, upper left panel), the model generally tracks the average longitudinal profile data at both high-slack and low-slack tide. Although no data were collected in the immediate vicinity of BCUA, both the model and data show an overall up-estuary and down-estuary displacement with the tide and a consistent decreasing pattern with increasing longitudinal distance from the source. The model underestimates the observed $\text{NH}_4\text{-N}$ distributions up-estuary from BCUA. This discrepancy likely arises from the fact that most of the freshwater inflow was actually contributed by BCUA during this dry-weather period, while the model assumes that all freshwater inflows occur at the head of tide. In any case, many of the salient features of the observed $\text{NH}_4\text{-N}$ distribution can be reproduced with this simple model (under dry-weather conditions) despite the apparent complexity of the HRE system.

LIMITATIONS DUE TO TEMPORAL SAMPLING RESOLUTION

To some degree, the selected water quality sampling frequency (every 2 or 3 h) limited the resolution of tidal variability measured in this study. A pertinent question is how frequently should water quality samples be collected to characterize semi-diurnal tidal variations (e.g., every 1, 2, 3 h, etc.)? There are few available guidelines on this issue, and the answer often depends on the ultimate use of the data as well as certain technical, logistical, and economic considerations.

To resolve M_2 tidal variability, it is necessary to sample at least as frequently as the well known Nyquist frequency, at least at quarter diurnal (6.21 solar hour or 6 lunar hour) intervals. In some cases, this necessary condition will not provide sufficient resolution to characterize a true sinusoidal

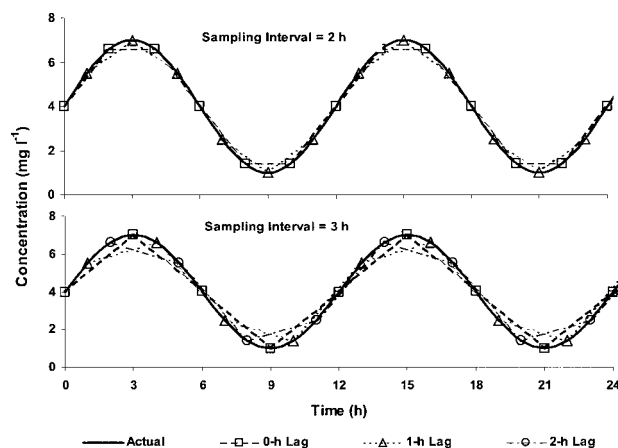


Fig. 8. Effect of under-sampling a pure sinusoidal variation at discrete intervals of 2 h (upper panel) and 3 h (lower panel). Varying time lags (0 h, 1 h or 2 h) of sampling are shown in each plot.

variation and a full tidal range. This issue is illustrated graphically in Fig. 8, which displays a hypothetical sinusoidal variation over time (solid curve) that is sampled discretely at fixed intervals of either 2 lunar hours (upper panel), or 3 lunar hours (lower panel), and from various starting points in time (0, 1, or 2 lunar hours after the start of the record).

To quantify these sampling errors, we computed corresponding relative errors every 15 lunar minutes over a complete cycle. Relative error is defined as the average magnitude of the differences between the two curves divided by the corresponding range in the observed concentrations. The relative errors associated with 2 lunar hour sampling (approximate) ranged from 5.3% to 5.9% and 3 lunar hour sampling ranged from 10.7% to 13.7%. The subject 2-h and 3-h sampling intervals are appropriate for first-order model analyses described above. The sinusoidal nature of the samples would be further distorted when the fixed sampling interval is increased above 3 lunar hours. In effect, peak concentrations may be underestimated (i.e., clipped) and curvature may be decreased, but this effect depends, in part, on the actual timing of the sampling relative to the concentration variation.

TIDAL VARIABILITY IN WATER QUALITY STATUS AND TREND ANALYSES

Tidal variability is not only an important consideration in designing monitoring programs, but also in assessing water quality status and detecting weak water quality trends. This is particularly the case in historically impaired water bodies (like the HRE) where improving trends are anticipated following pollution abatement programs. Few guide-

lines are available to determine the potential benefit of collecting water quality data at a fixed tidal phase (low tide) and whether resources should be focused on reducing other causes of variability (antecedent rainfall). Simple statistical analyses of data collected in the HRE readily provide insight to this matter.

Water quality status is usually assessed in terms of summary statistics, such as the estimated mean concentration and various percentile statistics. For example, a 95% confidence interval for the mean of a fairly large data set may be represented as:

$$\bar{C} \pm t_{0.975, n-1} \sqrt{\frac{S^2}{n}} \quad (7)$$

where \bar{C} is the sample mean concentration, S^2 is the sample variance, n is the sample size, $t_{0.975, n-1}$ is the value corresponding to the 0.975 percentile of the t -distribution with $n-1$ degrees of freedom, and $\sqrt{S^2/n}$ is the standard error of the mean. Tide and other external factors contribute to the sample variance and to the uncertainty in the estimate of a representative mean concentration.

A 95% confidence interval for the mean surface $\text{NH}_4\text{-N}$ concentration at station H5 was computed using the entire (unsorted) data set collected during the selected period (July 11–18, 1988). The computed sample variance for the entire series ($n = 49$) is $1.22 \text{ mg}^2 \text{ l}^{-2}$ (Table 3), and the corresponding confidence interval for the mean $\text{NH}_4\text{-N}$ concentration is $5.42 \pm 0.32 \text{ mg l}^{-1}$. The tide contributes to the computed variance and associated uncertainty in this estimate.

To reduce the tidal contribution to the variance, we partitioned the existing data set into the following more homogeneous subsets (strata): a low-slack stratum corresponding to data collected within ± 1 h of low-slack tide; a high-slack stratum corresponding to data collected within ± 1 h of high-slack tide, the remaining data collected during flood tide, and the remaining data collected during ebb tide. For each stratum, we computed a corresponding sample mean, sample variance, and confidence interval for the mean. Results indicate a reduction in the variance within these strata relative to the variance of the entire (unsorted) data set (Table 3). The computations yield divergent estimates of the mean concentration for the low-slack stratum versus the high-slack stratum (i.e., 3.95 ± 0.55 versus $6.06 \pm 0.40 \text{ mg l}^{-1}$). This result suggests that collection of data at a single tidal phase may introduce a significant tidal bias into the estimated mean concentration. An overall assessment of water quality status would require an analysis of data subsets collected at different tidal phases. Many ex-

TABLE 3. Effect of tidal sorting on calculation of confidence interval for mean surface $\text{NH}_4\text{-N}$ concentration at Station H5.

| Data Set or Stratum | Sample Size (n) | Sample Mean C (mg l ⁻¹) | Stratum Weight W_h | Sample Variance S^2 (mg ² l ⁻²) | $\sqrt{S^2/n}$ Standard Error (mg l ⁻¹) | $t_{975,n-1}$ | $\bar{C} \pm t_{975,n-1} \sqrt{S^2/n}$ Confidence Interval (mg l ⁻¹) |
|--|-----------------|-------------------------------------|----------------------|--|---|---------------|--|
| Entire data set (without poststratification) | 49 | 5.42 | | 1.22 | 0.16 | 2.01 | 5.42 ± 0.32 |
| Low-slack stratum (h = 1) | 12 | 3.95 | 0.16 | 0.76 | 0.25 | 2.20 | 3.95 ± 0.55 |
| High-slack stratum (h = 2) | 11 | 6.06 | 0.16 | 0.35 | 0.18 | 2.23 | 6.06 ± 0.40 |
| Flood stratum (h = 3) | 11 | 5.60 | 0.34 | 0.55 | 0.22 | 2.23 | 5.60 ± 0.50 |
| Ebb stratum (h = 4) | 15 | 6.01 | 0.34 | 0.36 | 0.15 | 2.14 | 6.01 ± 0.33 |
| Entire data set (with poststratification) | 49 | 5.55* | | 0.01** | 0.10 | 2.01 | 5.55 ± 0.21 |

* Weighted average of strat/means = $\sum_h W_h \bar{C}_h = (0.16)(3.95) + (0.16)(6.06) + (0.34)(5.60) + (0.34)(6.01) = 5.55 \text{ mg l}^{-1}$.

** Variance of the mean = $\sum_h [(W_h^2 S_h^2)/n_h] = [(0.16)^2/12](0.76) + [(0.16)^2/11](0.35) + [(0.34)^2/11](0.55) + [(0.34)^2/15](0.36) = 0.011 \text{ mg}^2 \text{ l}^{-2}$.

isting agency monitoring programs target a single tidal phase (low tide).

The partitioning of the existing data into non-overlapping strata (i.e., poststratification) allows for a more precise estimate of an overall mean concentration. Using poststratification techniques (Kish 1995), we computed an overall mean (and variance) that is essentially a weighted composite of the four strata means (and variances). We defined these averaging weights as the fraction of the 12.42-h tidal period associated with each stratum; 0.16 for the 2-h sampling window associated with both the low-slack and high-slack strata and 0.34 for both the flood-tide and ebb-tide strata. The resulting composite mean concentration (Table 3) is computed as the weighted average of the individual stratum means:

$$(0.16)(3.95) + (0.16)(6.06) + (0.34)(5.60) + (0.34)(6.01) = 5.55 \text{ mg l}^{-1} \quad (8)$$

The corresponding variance of the mean is essentially a composite of the individual strata variances (Kish 1995):

$$\frac{(0.16)^2}{12}(0.76) + \frac{(0.16)^2}{11}(0.35) + \frac{(0.34)^2}{11}(0.55) + \frac{(0.34)^2}{15}(0.36) = 0.011 \text{ mg}^2 \text{ l}^{-2} \quad (9)$$

where the coefficient of each term is the square of the corresponding strata weight divided by the corresponding strata sample size (Kish 1995). The corresponding standard error of the mean is the square root of 0.011 or 0.10 mg l⁻¹. The poststratification technique yields a confidence interval for the mean of $5.55 \pm 0.21 \text{ mg l}^{-1}$ (Table 3) that is slightly more precise than the interval obtained from the original (unsorted) data: $5.42 \pm 0.32 \text{ mg l}^{-1}$. The precision could be improved further with a proportionate sampling design (Kish 1995), with

34% of the samples collected during both the flood strata and ebb strata windows and 16% of the samples collected during both the low-slack and high-slack windows.

Tidal contributions to sample variance may be generalized as follows. Over an integer number of tidal cycles, the variance of a pure sinusoidal tidal constituent concentration variation is simply the square of its amplitude divided by two:

$$\begin{aligned} \text{Var} \left[C_T \sin \left(\frac{2\pi\pi}{T} \right) \right] &= \frac{1}{T} \int_0^T C_T^2 \sin^2 \left(\frac{2\pi\pi}{T} \right) dt \\ &\quad - \left[\frac{1}{T} \int_0^T C_T \sin \left(\frac{2\pi\pi}{T} \right) dt \right]^2 \\ &= \frac{C_T^2}{2} \quad (10) \end{aligned}$$

In the case of the $\text{NH}_4\text{-N}$ concentration data at station H5, the observed concentration range is 2–3 mg l⁻¹ (Fig. 4), corresponding to a concentration amplitude of 1.0–1.5 mg l⁻¹. From Eq. 10, the theoretical tidal contribution to the variance is about 0.50–1.13 mg² l⁻². This contribution is consistent (approximately) with the differences between the variance for the unsorted data set (1.22 mg² l⁻²) and the computed variances for each strata (0.76, 0.35, 0.55, and 0.36 mg² l⁻²). The poststratification of samples reduced the variance contributed by the tide.

Given the theoretical estimate for the tidal contribution to the sample variance (Eq. 10), its effect on the size of the confidence interval (for the mean concentration) for various combinations of sample size and sample variance can be assessed. Table 4 illustrates this effect (without poststratification) for a hypothetical data set having a moderate sample size ($n = 25$) and for varying nontidal components of the sample variance (assumed to

TABLE 4. Effect of variance due to tide on estimates for mean constituent concentration (water quality status). Sample size, n , equals 25 and $t_{0.975,24} = 2.064$. * Computed from Eq. 10.

| Nontidal Component of Sample Variance ($\text{mg}^2 \text{l}^{-2}$) | Tidal Amplitude C_T (mg l^{-1}) | Tidal Component of Sample Variance ($\text{mg}^2 \text{l}^{-2}$)* | Total Sample Variance S^2 ($\text{mg}^2 \text{l}^{-2}$) | $\sqrt{S^2/n}$ Standard Error (mg l^{-1}) | $\bar{C} \pm t_{0.975,24} \sqrt{S^2/n}$ Confidence Interval (mg l^{-1}) |
|---|--|---|---|--|--|
| 1 | 0.0 | 0.000 | 1.000 | 0.200 | $\bar{C} \pm 0.413$ |
| 1 | 0.5 | 0.125 | 1.125 | 0.212 | $\bar{C} \pm 0.438$ |
| 1 | 1.0 | 0.500 | 1.500 | 0.245 | $\bar{C} \pm 0.506$ |
| 1 | 1.5 | 1.125 | 2.125 | 0.292 | $\bar{C} \pm 0.602$ |
| 1 | 2.0 | 2.000 | 3.000 | 0.346 | $\bar{C} \pm 0.715$ |
| 2 | 0.0 | 0.000 | 2.000 | 0.283 | $\bar{C} \pm 0.584$ |
| 2 | 0.5 | 0.125 | 2.125 | 0.292 | $\bar{C} \pm 0.602$ |
| 2 | 1.0 | 0.500 | 2.500 | 0.316 | $\bar{C} \pm 0.653$ |
| 2 | 1.5 | 1.125 | 3.125 | 0.354 | $\bar{C} \pm 0.730$ |
| 2 | 2.0 | 2.000 | 4.000 | 0.400 | $\bar{C} \pm 0.826$ |

be 1 and 2 $\text{mg}^2 \text{l}^{-2}$). Results indicate that as the amplitude of the tidal variation increases, the size of the confidence interval increases marginally (along with the uncertainty in the estimate for the mean concentration). Tidal variability would confound the water quality status indicator (the mean concentration) only marginally for such moderate (or large) sample sizes. The confounding effect would likely be even smaller if either poststratification or proportionate sampling techniques were employed.

The confidence interval for the mean would be estimated by the sample mean $\pm 0.83 \text{ mg l}^{-1}$ for a water quality constituent having a tidal amplitude variation of 2 mg l^{-1} , a computed tidal component of the sample variance of 2 $\text{mg}^2 \text{l}^{-2}$, and an assumed nontidal component of the sample variance of 2 $\text{mg}^2 \text{l}^{-2}$ (Table 4, last row). Without the tidal variation, the corresponding interval would be the sample mean $\pm 0.58 \text{ mg l}^{-1}$. The difference ($\pm 0.83 \text{ mg l}^{-1}$ versus ± 0.58 or 0.25 mg l^{-1}) is likely small compared to typical mean $\text{NH}_4\text{-N}$ concentrations in an urbanized estuary (Fig. 5).

Another potential concern is that tidal variability may confound estimates for mean concentrations that are computed for different historical periods, masking weak temporal trends. A simple t -test may be applied to detect differences between two historical estimates for the mean concentration when the data are independent and have equal population variances. (Alternatively, nonparametric equivalent tests such as the Mann-Whitney U test may be applied). The critical t -test statistic is the ratio of the difference between two historical sample means and the standard error:

$$\frac{\bar{C}_1 - \bar{C}_2}{\sqrt{\frac{S_p^2}{n_1} + \frac{S_p^2}{n_2}}} = t_{0.975, n_1 + n_2 - 2} \quad (11)$$

where \bar{C}_1 and \bar{C}_2 are the two sample mean concen-

trations, n_1 and n_2 are the two sample sizes, and S_p^2 is the pooled sample variance (i.e., the average of the two sample variances, weighted by the respective sample sizes):

$$S_p^2 = \frac{(n_1 - 1)S_1^2 + (n_2 - 1)S_2^2}{n_1 + n_2 - 2} \quad (12)$$

Variability induced by the tide and other factors tends to increase the individual (and pooled) sample variances. In such cases, a larger difference between the historical sample mean concentrations would be needed in order to establish a significant trend (Eq. 11). This effect is illustrated in Table 5 for the special case of equal, moderate size samples (i.e., $n_1 = n_2 = 25$) and equal sample variances (i.e., $S_1^2 \approx S_2^2$). A 0.95- mg l^{-1} difference in sample means would be needed to establish a significant trend for constituents having a tidal amplitude variation of 2 mg l^{-1} and an assumed nontidal component of the sample variance of 2 $\text{mg}^2 \text{l}^{-2}$ (Table 5, last row). Without the tidal variation, a 0.67 mg l^{-1} difference in sample means would be required. Again, the tidal effect is only marginal for this moderate sample size case, suggesting that monitoring efforts should also be focused on reducing other causes of variability (e.g., antecedent rainfall).

The limited statistical analyses discussed above illustrate how data collection efforts that focus on a single tidal phase (low tide) may introduce a significant bias in estimates of water quality status indicators such as mean concentrations. Estimates of the overall mean concentration may be only marginally confounded by tidal variability if sample sizes are sufficiently large. The example trend analyses discussed above suggest that efforts should be made to minimize other causes of water quality variability (antecedent rainfall) and to collect sufficiently large samples to minimize the standard error. Only strong temporal trends may be detected.

TABLE 5. Effect of variance due to tide on *t*-test for differences in mean concentrations (water quality trends). Size of samples 1 and 2 equals 25 and $t_{0.975,48} = 1.68$ (i.e., $n_1 = n_2 = 25$).

| Nontidal Component of Sample Variance ($\text{mg}^2 \text{ l}^{-2}$) | Tidal Amplitude C_T (mg l^{-1}) | Tidal Component of Sample Variance ($\text{mg}^2 \text{ l}^{-2}$) | $\sqrt{2S^2/n}$ Standard Error (mg l^{-1}) | Minimum Significant Difference ($(C_1 - C_2)_{\min}$) (mg l^{-1}) |
|--|--|---|---|--|
| 1 | 0.0 | 0.000 | 0.283 | 0.48 |
| 1 | 0.5 | 0.125 | 0.300 | 0.50 |
| 1 | 1.0 | 0.500 | 0.346 | 0.58 |
| 1 | 1.5 | 1.125 | 0.412 | 0.69 |
| 1 | 2.0 | 2.000 | 0.490 | 0.82 |
| 2 | 0.0 | 0.000 | 0.400 | 0.67 |
| 2 | 0.5 | 0.125 | 0.412 | 0.69 |
| 2 | 1.0 | 0.500 | 0.447 | 0.75 |
| 2 | 1.5 | 1.125 | 0.500 | 0.84 |
| 2 | 2.0 | 2.000 | 0.566 | 0.95 |

Such observations may provide guidance for future data collection efforts in the HRE and similar effluent-dominated estuaries.

A comparison can be made to a more recent water quality data set collected in the HRE by the New Jersey Meadowlands Commission (NJMC; Konsevick 1999). From 1994–2002, NJMC collected these data at a frequency of once per season and at low tide (only). At a sampling location corresponding to Station H5, the mean of the 9 summer $\text{NH}_4\text{-N}$ concentrations sampled by NJMC is 3.71 mg l^{-1} ; the corresponding sample variance is $2.05 \text{ mg}^2 \text{ l}^{-2}$. The corresponding mean and variance of the approximate low-slack $\text{NH}_4\text{-N}$ data collected at Station H5 during the selected dry-weather period in 1988 are 3.95 mg l^{-1} (based on 12 samples) and $0.76 \text{ mg}^2 \text{ l}^{-2}$, respectively. From Eqs. 11 and 12, the corresponding test statistic of 0.48 falls below the critical 95% probability value (1.68), suggesting that the sample means are not different (i.e., no $\text{NH}_4\text{-N}$ trend detected). Detection of a significant trend would have required a larger difference between two historical sample mean concentrations and a reduced standard error by more frequent or targeted sampling.

ACKNOWLEDGMENTS

The authors thank the Bergen County Utilities Authority (BCUA) for sponsoring the collection of data used in this analysis. The authors appreciate the recent data provided by the New Jersey Meadowlands Commission (Ed Konsevick, laboratory manager) and the Rutgers University Meadowlands Environmental Research Institute (Dr. Kirk Barrett, science director). We are grateful to all of the reviewers for providing helpful and timely comments.

LITERATURE CITED

BROSNAN, T. M. AND M. L. O'SHEA. 1996. Long-term improvements in water quality due to sewage abatement in the lower Hudson River. *Estuaries* 19:890–900.

CLOERN, J. E., T. M. POWELL, AND L. M. HUZZEY. 1989. Spatial and temporal variability in South San Francisco Bay (USA). II. Temporal changes in salinity, suspended sediments, and

phytoplankton biomass and productivity over tidal time scales. *Estuarine, Coastal and Shelf Science* 28:599–613.

GEYER, W. R. AND R. P. SIGNELL. 1992. A reassessment of the role of tidal dispersion in estuaries and bays. *Estuaries* 15:97–108.

GOODRICH, D. M. 1988. On meteorologically induced flushing in three U.S. East Coast estuaries. *Estuarine, Coastal and Shelf Science* 26:111–121.

HARLEMAN, R. F. 1971. One-dimensional models. Estuarine Modeling: An Assessment. Tracor Inc. and U.S. Environmental Protection Agency, Water Quality Office, Washington D.C., Project No. 16070DZV.

HUBERTZ, E. D. AND L. B. CAHOON. 1999. Short-term variability of water quality parameters in two shallow estuaries of North Carolina. *Estuaries* 22:814–823.

KELLER, A. A., K. R. HINGA, AND C. A. OVIATT. 1990. New York–New Jersey Harbor estuary program module 4: Nutrients and organic enrichment. Marine Ecosystems Research Laboratory, Graduate School of Oceanography, University of Rhode Island, Narragansett, Rhode Island.

KISH, L. 1995. Survey Sampling. John Wiley and Sons, Inc., New York.

KONSEVICK, E. 1999. Hackensack River Water Quality (Draft). Hackensack Meadowlands Development Commission Environmental Operations Research Laboratory, Lyndhurst, New Jersey.

NAJARIAN ASSOCIATES. 1990. Impact analysis of sewage treatment plant discharges on the water quality of the lower Hackensack River. Report for Bergen County Utilities Authority, Little Ferry, New Jersey.

SANDERSON, P. G. AND D. M. TAYLOR. 2003. Short-term water quality variability in two tropical estuaries, Central Sumatra. *Estuaries* 26:156–165.

SHARPLES, J. AND J. H. SIMPSON. 1993. Periodic frontogenesis in a region of freshwater influence. *Estuaries* 16:74–82.

SIMPSON, J. H., J. BROWN, J. MATTHEWS, AND G. ALLEN. 1990. Tidal straining, density currents, and stirring in the control of estuarine stratification. *Estuaries* 13:125–132.

SQUIBB, K. S., J. M. O'CONNOR, AND T. J. KNEIP. 1991. New York/New Jersey harbor estuary program module 3.1: Toxics characterization. Institute of Environmental Medicine, New York University Medical Center, Tuxedo, New York.

UNCLES, R. J. 2002. Estuarine physical processes research: Some recent studies and progress. *Estuarine, Coastal and Shelf Science* 55:829–856.

U.S. ENVIRONMENTAL PROTECTION AGENCY (U.S. EPA). 1983. Methods for Chemical Analysis of Water and Wastes. EPA 600-3-83-020. Cincinnati, Ohio.

Received, March 24, 2004

Revised, June 24, 2004

Accepted, June 29, 2004